OPTO-ELECTRONICS REVIEW **20**(2), 194–199

DOI: 10.2478/s11772-012-0024-z

Sub-THz radiation room temperature sensitivity of long-channel silicon field effect transistors

F. SIZOV*, A. GOLENKOV, D. BUT, M. SAKHNO, and V. REVA

Institute of Semiconductor Physics, 41 Nauki Ave., 03028 Kiev, Ukraine

Room temperature operating n-MOSFETs (n-type metal-oxide silicon field effect transistors) used for registration of sub-THz (sub-terahertz) radiation in the frequency range ν = 53–145 GHz are considered. n-MOSFETs were manufactured by 1-µm Si CMOS technology applied to epitaxial Si-layers (d ≈15 µm) deposited on thick Si substrates (d = 640 µm). It was shown that for transistors with the channel width to length ratio W/L = 20/3 µm without any special antennas used for radiation input, the noise equivalent power (NEP) for radiation frequency ν ≈76 GHz can reach NEP ~6×10^{-10} W/Hz$^{1/2}$. With estimated frequency dependent antenna effective area S_{est} for contact wires considered as antennas, the estimated possible noise equivalent power NEP_{pos} for n-MOSFET structures themselves can be from ~15 to ~10^3 times better in the specral range of ν ~55–78 GHz reaching NEP_{pos} ~10^{-12} W/Hz$^{1/2}$.

Keywords: n-MOSFETs, sub-THz detectors, NEP.

1. Introduction

In THz spectra technologies (ν ~0.1–10 THz), design of uncooled effective detectors attracts attention because of the needs for wide potential applications in vision systems spectroscopy, medicine, security, etc. For example, in vision or security applications this is conditioned with the fact that THz/sub-THz radiation being non-ionizing at the same time is some kind of alternative to X-ray technologies as many materials (plastics, cloths, paper-boards, etc.) are also transparent and in THz/sub-THz spectra region.

Today, there exist quite a lot of different types of THz/sub-THz detectors, the most sensitive ones are deeply cooled to cryogenic or sub-K operation temperatures [1]. Their *NEP* in some spectral THz/sub-THz regions at low background level reaches *NEP* ~10^{-16}–10^{-19} W/Hz$^{1/2}$. Most of uncooled THz/sub-THz detectors are not sensitive enough (*NEP* ~10^{-8}–10^{-9} W/Hz$^{1/2}$) or are not capable for integration into arrays to be used, e.g. in real time vision systems. In order to be widely used in THz/sub-THz technologies, the detectors should be not only relatively sensitive but also un-cooled or slightly cooled (not deeper than to liquid nitrogen temperature T = 77 K) and capable for integration into arrays with readout electronics. These require further improvements in their sensitivity at the elevated, compared to sub-K operation temperatures, and capability integration within the developed integration technologies. That will make the THz/sub-THz systems much less complicated and bulky.

Among the number of various detectors proposed and realized for THz/sub-THz spectral region in recent two decades, the concept of THz detection based on excitation of plasma waves in two-dimensional electron gas of Si FETs integrated with ROICs (readout devices) seems to be one of the most attractive, as it makes possible the development of the large-scale integrated devices based on conventional integration technologies (including on-chip antenna integration).

Use FETs as generators or detectors of THz radiation and explanation the detection phenomena in these devices were proposed in Refs. 2 and 3. One of the first presentation of FETs THz/sub-THz detector was made in Ref. 4. Later on (see, e.g. Ref. 5–8), it was shown that these detectors can reach *NEP* values comparable with the best conventional room-temperature devices with *NEP* ~$(1–30)\times10^{-11}$ W/Hz$^{1/2}$, but to reach such favourable *NEP* values these devices required special kind of micro-antennas optimized for spectral band selected (here in the frequency range of ν ~300–650 GHz). In these investigations, FETs were manufactured according to better designed rules (0.25, 0.13 or 0.065 µm) CMOS technologies compared and investigated here.

2. Experiment

As detector structures to sub-THz radiation in the frequency range of ν = 53–145 GHz here were used Si n-MOSFETs with channel width to length ratio W/L = (1–20)/(1–20) µm, that were manufactured by 1-µm CMOS technology applied to epitaxial layers with the resistivity ρ ≈35 Ω · cm and the thickness d ≈15 µm. The epitaxial layers were grown on

*e-mail: sizov@isp.kiev.ua

bulk Si substrates (thickness d = 640 μm) with $\rho \approx 0.01\ \Omega \cdot$ cm. Schematic representation of n-channel FET is shown in Fig. 1. Figure 2 shows one of the linear arrays investigated with two FETs zoomed (right part). The considered structures had common gate and source contacts and separate drain contacts. At room temperature, the threshold voltages in these MOSFETs were within the V_{th} = 0.56–0.7 V. As sub-THz emitters the backward-wave oscillators (BWOs) were used. No special micro-antennas were applied to this kind of detectors as, e.g. in Ref. 9, where the sensitivity S_V = 2 V/W was obtained at ν = 200 GHz and at zero bias drain current applied to room-temperature strained-Si modulation doped FETs.

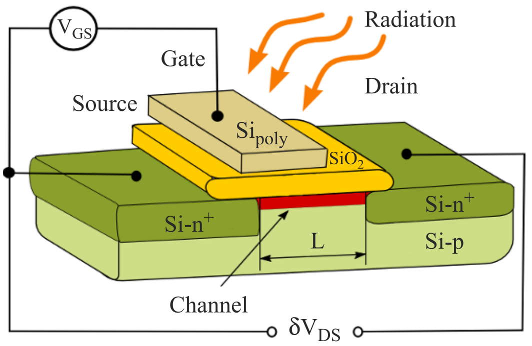

Fig. 1. Schematic of n-channel FET. V_{GS} is the gain-source voltage, δV_{DS} is the drain voltage under radiation.

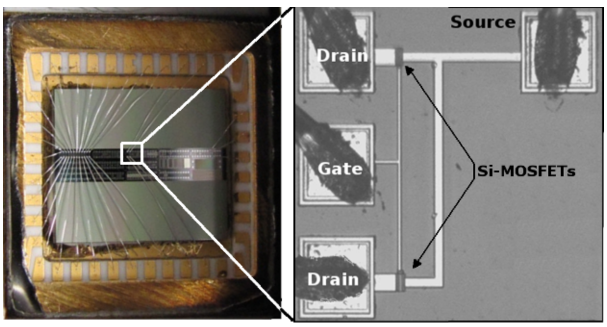

Fig. 2. One of linear array of Si n-MOSFETs in ceramic case.

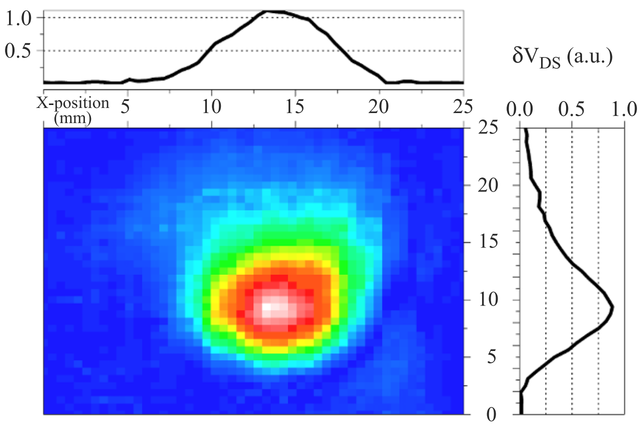

Fig. 3. Relative radiation power distribution mapped with Si n-MOSFET investigated, ν = 127 GHz.

The power density at detector displacement in the spectral range ν ~55–78 GHz was W_{beam} ~2 m W/cm^2 and in the spectral range ν ~127–145 GHz it was W ~8 m W/cm^2. Power relative distribution at FET structures displacement, obtained by one of FETs used as detector, is shown in Fig. 3. Modulated with the frequency $f \approx$150–1500 Hz, radiation was focused onto the structures by parabolic mirror, and the drain-source voltage δV_{DS} induced under the radiation was measured using a lock-in amplifier technique.

3. Model and results

In Fig. 4, at room temperature, it is shown the signal dependence δV_{DS} at drain contact as a function of the gate voltage V_{GS}. The phenomenon of δV_{DS} appearance is connected with plasma waves in FET channel. When THz/sub-THz radiation power is introduced to FET (e.g. between gate and source), the ac THz voltage modulates simultaneously the carrier density and the carrier drift velocity in the FET channel [3]. The observed detection is due to nonlinear properties of FETs which is the reason for rectification of an AC current conditioned by THz/sub-THz radiation. Hereupon, in long channels, a dc voltage response to δV_{DS} between source and drain arises which is proportional to THz power received by FET [10,11]. For high carrier mobility FET short channels (e.g. III-V low-temperature ones), THz field can induce resonant plasma waves that can lead to a detection resonant at some radiation frequencies.

In silicon at room or cryogenic temperatures, plasma waves are usually over-damped in short part of channels leading to a non-resonant detection that can be rather broadband when appropriate antennas are used for a radiation input. In this case, the THz radiation causes only a carrier density perturbation that decays exponentially with distance and is constant in long (L > 0.05–0.1 μm) Si channels [5,10,12]. Non-resonant detection also can be explained alternatively by the model of distributed resistive self-mixing [6,10–12].

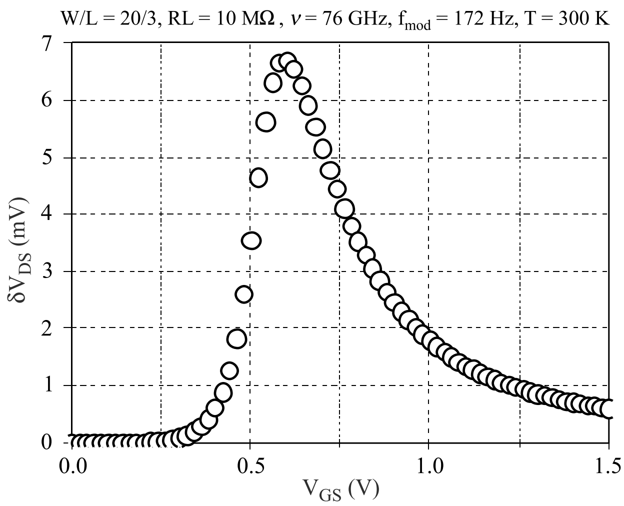

Fig. 4. δV_{DS} signals in function of gate voltage V_{GS}. R_L is the load resistance, f is the modulation frequency.

For arising the DC δV_{DS} voltage, the asymmetry between the source and the drain should exist. The most obvious condition for it is to insert an antenna between the gate and the source that is needed to introduce the radiation power into the FET channel. However, the DC voltage can arise because of asymmetric design of busses in the silicon substrate to source (drain) and contact pads to them, wire-contacts to pads, etc. And when antennas are absent that can lead to compensation powers introduced through the *S-G* or *D-G* inputs and the small δV_{DS} level voltages observed and that even can lead to changes of the current direction in FET channels.

For a long transistor channel case ($L > 0.1$ μm), the transistor drain rectified signal voltage response δV_0 is [3,10]

$$\delta V_0 = \frac{V_a^2}{4(V_{GS} - V_{TH})}, \tag{1}$$

where V_{GS} is the gate voltage bias, V_{TH} is the transistor threshold voltage, V_a is the amplitude of an input signal in the channel under the THz radiation [$V_{in} = V_a \sin(\omega t)$] influence. Equation (1) is valid for linear regime of transistor operation when $V_{DS} < V_{GS} - V_{TH}$ and $V_{GS} - V_{TH} > \eta k_B T/e^-$, where η ~1.5–2 is the transistor ideality factor, k_B is the Boltzmann constant, and e^- is the electron charge. Here V_{DS} is the drain voltage (bias) that in these experiments was taken zero.

As the signal direct component δV_0 is formed at short part near the source of transistor (< 0.1 μm) [5,10–12] and the channel lengths of the investigated transistors were within 1 and 20 microns and the rest of the channel is simply a resistor, the signals at transistor drain δV_{DS} differs from the signal DC voltage component δV_0. Since the channel resistance R_{CH} and the external load impedance Z_L form the voltage divider [13], the relation between δV_0 and δV_{DS} can be written as

$$\begin{aligned} \delta V_0 &= R_{CH}\,\delta I_{DS} + Z_L\,\delta I_{DS}, \\ Z_L &= R_L \| X_{CL}, \qquad , \\ X_{CL} &= -\frac{i}{2\pi f_{\text{mod}} C_L}, \end{aligned} \tag{2}$$

where δI_{DS} is the current response on THz irradiation, R_L is the load resistance, X_{CL} is the load capacitance, C_L is the load capacity, and f_{mod} is the modulation frequency.

The maximum current δI_0 which can be estimated with the load impedance value $Z_L = 0\ \Omega$, is $\delta I_0 = \delta V_0/R_{CH}$.

The importance of taking into account the channel resistance is illustrated by estimations of channel resistance and drain current δI_{DS} dependences for FETs *vs.* V_{GS} voltage using the voltage divider model that are shown in Fig. 5 for transistors with different load resistances at ν = 127 GHz. For ROICs to be used with FET-detector arrays, it is important to get relatively large, at least several *nA* signal currents δI_{DS}.

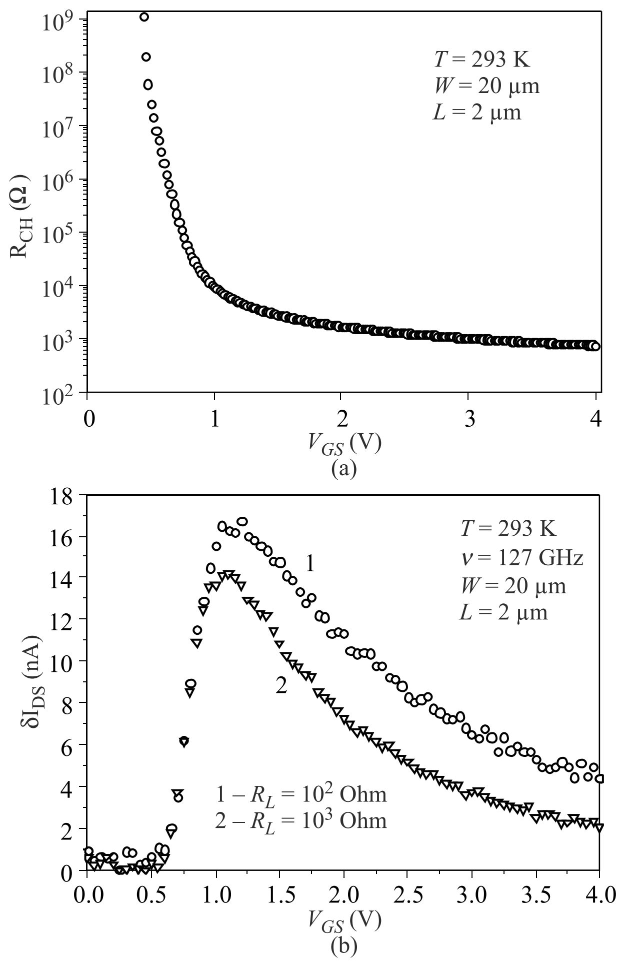

Fig. 5. Estimations of channel resistance (a) and signal drain current δI_{DS} under the radiation (ν = 127 GHz, the radiation power density W ~8 mW/cm^2) (b) *vs.* V_{GS} voltage using the voltage divider model for one of n-MOSFET structures.

4. Sensitivity and *NEP* discussion

One of the most important parameters that characterize detectors is *NEP*. It can be determined as $NEP = V_{noise}/S_V$ (W/Hz$^{1/2}$), where V_{noise} is the detector noise, and the voltage sensitivity $S_V = \delta V_{DS}/W$. Here δV_{DS} is the DC response, and W is the THz/sub-THz radiation power falling down on detector.

The dominant noise in FETs in the case considered $V_{DS} = 0$ is the thermal noise in FET channel [5,7]: $V_{noise} = \sqrt{4k_B T R_{CH}}$. Therefore the detector *NEP* can be estimated as

$$NEP = \sqrt{4k_B T R_{CH}} \,/ S_v. \tag{3}$$

FET area is much less than the diffraction limited Airy disk diameter $A_{dif} \approx 2.44\lambda_0(f/D)$ of THz/sub-THz wave at which ≈84% of incident power are localized for detectors without antennas. Here, f is the focal length of the optical system, D is the aperture diameter, λ_0 is the incident radiation wavelength (in air). As in this spectral region for a radiation input different kind of antennas are applied, some kind of "active" or "effective" antenna areas are used, e.g., $S_{\lambda act} = \lambda_0^2/4$ [5,9], or "physical detector size" (pitch) [7, 11]. $(S_{\lambda act})^{1/2}$ or pitch can be less than A_{dif} (also taking into account that frequently $f/D > 1$) that increases estimations of S_V and decreases (makes better) estimations of *NEP*.

To find out the antenna loaded detector *NEP* upper limit for given wavelength one should take into account the effective antenna area S_λ (sensitivity $S_V \sim S_\lambda = (\lambda^2/4\pi)G$) that in the case of antenna with conduction-dielectric losses can be less compared to max effective antenna area that is determined by [14,15]

$$S_\lambda = \frac{\lambda^2}{4\pi} G, \tag{4}$$

where λ is the wavelength in semiconductor or dielectric substrate, G is the gain coefficient that is dependent on the radiation frequency, the angles between normal detector surface and radiation direction of propagation, the radiation polarization relative to antenna, the dielectric constant of substrate, their thickness and conductivity, the antenna's shape, etc. Frequently it is taken $G = 1$.

In such an approximation ($G = 1$) for FET structures (W/L = 20/3 μm) measured here at room temperature at $\nu \approx 76$ GHz (see Fig. 4) the voltage sensitivity S_V and *NEP* were estimated: $S_V \sim 280$ V/W and $NEP \sim 6\times10^{-10}$ W/Hz[12] (see also Fig. 6, upper curve). In the experiments with this detector the load resistance was $R_L = 10$ MΩ, the modulation frequency $f = 172$ Hz, the gate voltage $V_{GS} = 0.63$ V, and the estimated channel resistance $R_{CH} \approx 2$ MΩ. These data of S_V and *NEP* were obtained without any special antennas incorporated (as antennas serve the contact wires). They correspond to parameters of many other un-cooled THz/sub-THz detectors [1,16] but really they are underestimated as no special antennas were applied.

In order to take into account in *NEP* estimations the contacts-wires and pads used as antennas [17] with effective

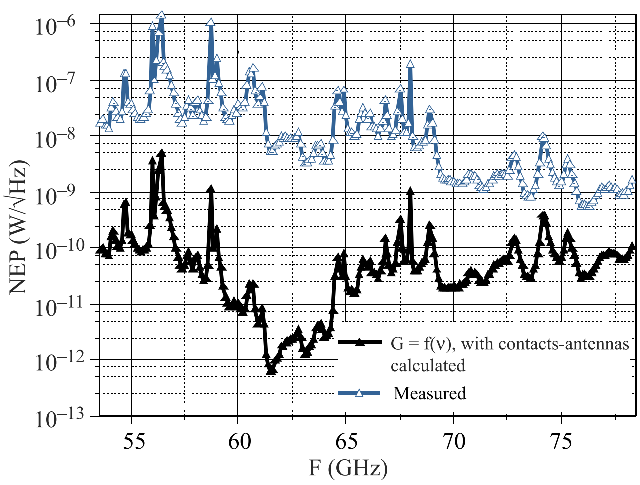

Fig. 6. Typical NEP frequency dependences of Si n-MOSFET structure (W/L = 20/2 μm) at room temperature.

areas here was carried out the modelling of influence of wires-antennas on the sensitivity spectral characteristics of n-MOSFET structures investigated. In estimations Au 30 μm wires were accepted as ideal conductors and Si substrate was taken as an infinite one. It was shown that because of thick Si substrates and wires-antennas configuration in this spectral range the antenna effective area S_{est} values are low. But as the sensitivity $S_V \sim S_{est} = (\lambda^2/4\pi)G$ the radiation collection area and the sensitivity are much smaller that it can be in the case of "good" antennas.

These low S_{est} values estimated do not allow to realize potentially [18] high sensitivity S_V values ($S_V = \delta V_{DS}/W$) and low *NEP* values ($NEP = V_{noise}/\delta V_{DS} \sim V_{noise}/(\lambda^2/4\pi)G$) of Si n-MOSFET sub-THz detectors (the lower *NEP*, the more sensitive detector). The higher will be the antenna effective area, the higher will be the power input into the channel and consequently the higher will be the sensitivity S_V and the smaller the *NEP* values. For estimations of possible NEP_{pos} using the NEP_{exp} values obtained from the experimental data $NEP_{pos} = NEP_{exp}S_{est}(\nu)$ (see Fig. 6, bottom curve) were calculated.

These electromagnetic simulation estimations of $S_{est}(\nu)$ were made for Si n-MOSFETs on thick silicon substrates and wires-antennas orientation shown in Fig. 7 for $\nu = 131$ and 143 GHz in far field approximation with the help of all-wave technique finite element method (FEM) that is frequently used successfully for calculations of antenna parameters taking into account the substrate parameters. These estimations have shown that radiation is coupling inefficiently in this spectral range by contacts-wires, partly due to the overcompensation of the radiation power introduced through the *S-G* and *D-G* inputs. The proper antenna design can lead to much more efficient radiation coupling to MOSFET channel resulting in much more sensitive detector.

The influence of contacts-wires for FET structures is noticeable and determinative for the angle signal dependences when micro-antennas are absent in a spectral range of $\nu \sim 40$–145 GHz (see Fig. 7, for $\nu = 131$ and 143 GHz). As one can see, the long axis orientation of the lobes along the contact-wires depends on radiation frequency and is not obviously dependent on the radiation electrical vector **E**-polarization. This is due to the processes of multiple reflections and attenuation of the radiation in a rather thick silicon substrate. Asymmetry of the lobes in Fig. 7 is conditioned by $\theta \sim 5°$ angle deviation between the direction of radiation propagation and the normal to the sample surface.

The results obtained indicate that uncooled Si-MOSFET structures for detectors of THz/sub-THz radiation even manufactured with not very moderate CMOS technologies (e.g. here 1 μm design rules technology was applied) potentially are high-sensitive un-cooled sensors with inherent parameters comparable or exceeding the parameters of the best un-cooled detectors for THz/sub-THz spectral range but for realization of such parameters the proper antenna design to increase the antenna effective area values should

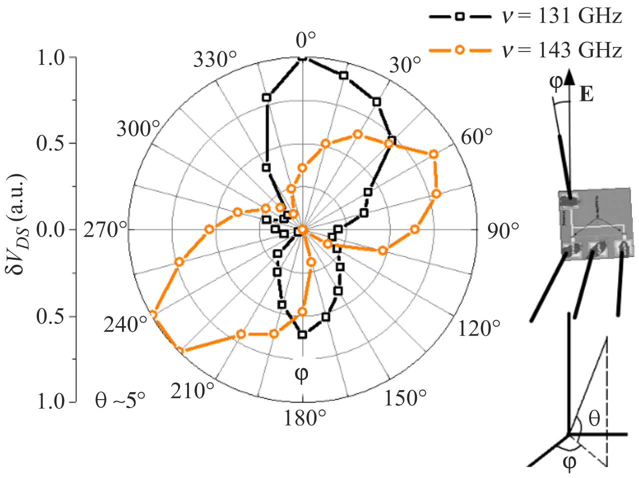

Fig. 7. Photoresponse angular dependences of n-MOSFET structure at different radiation frequencies. The wires-contacts disposition is shown in the inset. φ is the angle between the wire-contact and **E** is the polarization of the radiation, θ is the angle between the direction of radiation propagation and the normal to the sample surface.

be used. One of the possibilities to increase the antenna effective area values is thinning of not very optimal for these purposes Si substrates (because of high losses due to the high dielectric permittivity ε in silicon and substrate thickness). That was shown, e.g. in Ref. 7, for n-MOSFET detectors on Si substrates with thickness $d = 125$ μm. Also it can be realized by using substrates with lower ε values on which antennas with high directivity and gain can be formed [8]. FET detectors cited in these papers were manufactured according to better design rules (0.13 and 0.065 μm) than used here.

Still in these cited papers there were not achieved potentially high parameters of MOSFET THz detectors themselves that can be obtained for optimized substrates and antennas design with high antenna effective area values, and these parameters remain at least from 2 to 3 orders worth of the ultimate estimations ($NEP_{ult} \approx (2–5)\times 10^{-15}$ W/Hz$^{1/2}$) for uncooled detector *NEP*'s limited only by power fluctuations of the background radiation for diffraction limited beams [16]. Realization for n-MOSFETs, the values of $NEP < 10^{-12}$ W/Hz$^{1/2}$ can pave the way towards focal plane arrays for passive vision but, in fact, at present n-MOSFET uncooled detectors can be used only in active vision systems.

n-MOSFET structures as detectors are more complicated as radiation detectors compared to, e.g., bolometers with only two contacts. In n-MOSFET structures, there are four contacts (or, at least, three ones). Because of the contacts-wires presence and buses in Si substrate (especially for FET detectors with readouts), the radiation power in sub-THz region is introduced both between source-gate and drain-gate contacts even in the case when the special antennas are incorporated between *S-G* contacts.

Acknowledgements

This work has been partially supported by the Ukrainian National Foundation Grant N Φ 40/54-2011.

References

1. F. Sizov, "THz radiation sensors", *Opto-Electron. Rev.* **18**, 10–36 (2010).
2. M. Dyakonov and M. Shur, "Shallow water analogy for a ballistic field effect transistor. New mechanism of plasma wave generation by dc current", *Phys. Rev. Lett.* **71**, 24652468 (1993).
3. M. Dyakonov and M. Shur, "Detection mixing, and frequency multiplication of terahertz radiation by two-dimensional electronic fluid", *IEEE Trans. Electr. Devices* **43**, 380–387 (1996).
4. W. Knap, F. Teppe, Y. Meziani, N. Dyakonova, J. Lusakowski, F. Boeuf, T. Skotnicki, D. Maude, S. Rumyantsev, and M. S. Shur, "Plasma wave detection of sub-terahertz and terahertz radiation by silicon field-effect transistors", *Appl. Phys. Lett.* **85**, 675–677 (2004).
5. R. Tauk, F. Teppe, S. Boubanga, D. Coquillat, W. Knap, Y. Meziani, C. Gallon, F. Boeuf, T. Skotnicki, C. Fenouillet--Beranger, D.K. Maude, S. Rumyantsev, and M.S. Shur, "Plasma wave detection of terahertz radiation by silicon field effect transistors: responsivity and noise equivalent power", *Appl. Phys. Lett.* **89**, 253511 (2006).
6. E. Öjefors, U.R. Pfeiffer, A. Lisauskas, and H.G. Roskos, "A 0.65 THz focal-plane array in a quarter-micron CMOS process technology", *IEEE J. Solid-St. Circuits* **44**, 1968–1976 (2009).
7. F. Schuster, D. Coquillat, H. Videlier, M. Sakowicz, F. Teppe, L. Dussopt, B. Giffard, T. Skotnicki, and W. Knap, "Broadband terahertz imaging with highly sensitive silicon CMOS detectors", *Opt. Express* **19**, 7827–7832 (2011).
8. E. Öjefors, N. Baktash, Y. Zhao, R. Al Hadi, H. Sherry, and U. Pfeiffer, "Terahertz imaging detectors in a 65-nm CMOS SOI technology", *Proc. the 37th European Conf. Solid-St. Circuits*, Seville, 486–489 (2010).
9. S.L. Rumyantsev, K. Fobelets, D. Veksler, T. Hackbarth, and M. Shur, "Strained-Si modulation doped field effect transistors as detectors of terahertz and sub-terahertz radiation", *Semicond. Sci. Technol.* **23**, 105001 (2008).
10. W. Knap, M. Dyakonov, D. Coquillat, F. Teppe, N. Dyakonova, J. Lusakowski, K. Karpierz, M. Sakowicz, G. Valusis, D. Seliuta, I. Kasalynas, A. El Fatimy, Y.M. Meziani, and T. Otsuji, "Field effect transistors for terahertz detection: Physics and First Imaging Applications", *J. Infrared Milli. Terahz. Waves* **30**, 1319–1337 (2009).
11. A. Lisauskas, D. Glaab, H.G. Roskos, E.U. Oejefors, and R. Pfeiffer, "Terahertz imaging with Si MOSFET focal-plane arrays", *Proc. SPIE* **7215**, 72150J–11 (2009).
12. A. Lisauskas, U. Pfeiffer, E. Öjefors, P.H. Bolivar, D. Glaab, and H.G. Roskos, "Rational design of high-responsivity detectors of terahertz radiation based on distributed self-mixing in silicon field-effect transistors", *J. Appl. Phys.* **105**, 114511 (2009).
13. M. Sakowicz, M.B. Lifshits, O.A. Klimenko, F. Schuster, D. Coquillat, F. Teppe, and W. Knap, "Terahertz responsivity of

field effect transistors versus their static channel conductivity and loading effects", *J. Appl. Phys.* **110**, 054512 (2011).
14. C.A. Balanis, *Antenna Theory: Analysis and Design*, Wiley, New Jersey, 2005.
15. *Antenna Engineering Handbook*, edited by J.L. Volakis, McGraw-Hill, New York 2007.
16. F. Sizov, V. Reva, A. Golenkov, and V. Zabudsky, "Un-cooled detectors challenges for THz/sub-THz arrays imaging", *J. Infrared Milli. Terahz. Waves,* **32**, 1192–1206 (2011).
17. M. Sakowicz, J. Lusakowski, K. Karpierz, M. Grynberg, W. Knap, and W. Gwarek, "Polarization sensitive detection of 100 GHz radiation by high mobility field-effect transistors", *J. Appl. Phys.* **104**, 024519 (2008).
18. Y. Deng and M.S. Shur, "Electron mobility and terahertz detection using silicon MOSFETs", *Solid-St. Electr.* **47**, 1559–1563 (2003).